Invariance of polarized reflectance measured at the top of atmosphere by PARASOL satellite instrument in the visible range with marine constituents in open ocean waters

Tristan Harmel, Malik Chami

Invariance of polarized reflectance measured at the top of atmosphere by PARASOL satellite instrument in the visible range with marine constituents in open ocean waters

Tristan Harmel[1*] and Malik Chami[1]

[1]*Université Pierre et Marie Curie-Paris6, Laboratoire Océanographie de Villefranche, 06230 Villefranche sur Mer, France ; CNRS, Laboratoire Océanographie de Villefranche Villefranche sur Mer, France*
**Corresponding author: harmel@obs-vlfr.fr*

Abstract: The influence of oceanic constituents on the polarized reflectance measured at the top of atmosphere (TOA) over open ocean waters in one visible band is investigated. First, radiative transfer modelling is used to quantify the effects of biomass concentration on the TOA polarized signal for a wide range of observation geometries. The results showed that the TOA polarized reflectance remains insensitive to variations in the chlorophyll *a* concentration whatever the geometrical conditions in oligotrophic and mesotrophic waters, which represent about 90% of the global ocean. The invariance of the polarized signal with water content is explained by the prevailing influence of both atmospheric effects and skylight reflections at the sea surface on the polarization state of the radiation reaching the top of atmosphere level. The simulations also revealed that multidirectional and polarized TOA reflectances obtained in the visible spectrum are powerful tools for the discrimination between the aerosol optical properties. In the second part of the paper, the theoretical results are rigorously validated using original multiangle and polarized measurements acquired by PARASOL satellite sensor, which is used for the first time for ocean color purposes. First, a statistical analysis of the geometrical features of PARASOL instrument showed that the property of invariance of the TOA polarized reflectance is technically verified for more than 85% of viewed targets, and thus, indicating the feasibility of separating between the atmospheric and oceanic parameters from space remotely sensed polarized data. Second, PARASOL measurements acquired at regional and global scales nicely corroborated the simulations. This study also highlighted that the radiometric performance of the polarized visible wavelength of PARASOL satellite sensor can be used either for the aerosol detection or for atmospheric correction algorithms over open ocean waters regardless of the biomass concentration.

OCIS codes: (120.0280) Remote sensing and sensors; (010.1285) Atmospheric correction; **(**010.0010) Atmosphere and ocean optics; (260.5430) Polarization; (010.5620) Radiative transfer.

References and links

1. P. Y. Deschamps, F. M. Breon, M. Leroy, A. Podaire, A. Bricaud, J. C. Buriez, and G. Seze, "The Polder Mission - Instrument Characteristics And Scientific Objectives," IEEE Trans. Geosci. Remote Sens. **32**, 598-615 (1994).
2. S. Mukai, I. Sano, and T. Takashima, "Investigation of atmospheric aerosols based on polarization measurements and scattering simulations," Opt. Rev. **3**, 487-491 (1996).
3. M. I. Mishchenko and L. D. Travis, "Satellite retrieval of aerosol properties over the ocean using polarization as well as intensity of reflected sunlight," J. Geophys. Res. **102**, 16989-17013 (1997).

#91057 - $15.00 USD Received 20 Dec 2007; revised 6 Feb 2008; accepted 13 Feb 2008; published 15 Apr 2008

4. G. Miecznik, R. Illing, S. Petroy, and I. N. Sokolik, "Sensitivity metric approach for retrieval of aerosol properties from multiangular and multispectral polarized radiances," Appl. Opt. **44**, 4186-4204 (2005).
5. F. M. Breon, J. L. Deuze, D. Tanre, and M. Herman, "Validation of spaceborne estimates of aerosol loading from Sun photometer measurements with emphasis on polarization," J. Geophys. Res. **102**, 17187-17195 (1997).
6. E. Boesche, P. Stammes, T. Ruhtz, R. Preusker, and J. Fischer, "Effect of aerosol microphysical properties on polarization of skylight: sensitivity study and measurements," Appl. Opt. **45**, 8790-8805 (2006).
7. P. Goloub, F. Waquet, J. L. Deuze, M. Herman, F. Auriol, J. F. Leon, J. Y. Balois, C. Verwaerde, and D. Tanre, "Development of a multispectral polarimeter dedicated to aerosol characterization - Preliminary results," IGARSS 2003: IEEE Int. Geosci. Remote Sens. Symp., Vols I - Vii, Proceedings, 2164-2166 (2003).
8. M. Herman, J. L. Deuze, A. Marchand, B. Roger, and P. Lallart, "Aerosol remote sensing from POLDER/ADEOS over the ocean: Improved retrieval using a nonspherical particle model," J. Geophys. Res. **110**(2005).
9. A. Vermeulen, C. Devaux, and M. Herman, "Retrieval of the scattering and microphysical properties of aerosols from ground-based optical measurements including polarization. I. Method," Appl. Opt. **39**, 6207-6220 (2000).
10. B. Fougnie, G. Bracco, B. Lafrance, C. Ruffel, O. Hagolle, and C. Tinell, "PARASOL in-flight calibration and performance," Appl. Opt. **46**, 5435-5451 (2007).
11. O. Hagolle, P. Goloub, P. Y. Deschamps, H. Cosnefroy, X. Briottet, T. Bailleul, J. M. Nicolas, F. Parol, B. Lafrance, and M. Herman, "Results of POLDER in-flight calibration," IEEE Trans. Geosci. Remote Sens. **37**, 1550-1566 (1999).
12. M. Chami, R. Santer, and E. Dilligeard, "Radiative transfer model for the computation of radiance and polarization in an ocean-atmosphere system: polarization properties of suspended matter for remote sensing," Appl. Opt. **40**, 2398-2416 (2001).
13. J. Chowdhary, B. Cairns, and L. D. Travis, "Case studies of aerosol Retrievals over the ocean from multiangle, multispectral photopolarimetric remote sensing data," J. Atmos. Sci. **59**, 383-397 (2002).
14. J. Chowdhary, B. Cairns, and L. D. Travis, "Contribution of water-leaving radiances to multiangle, multispectral polarimetric observations over the open ocean: bio-optical model results for case 1 waters," Appl. Opt. **45**, 5542-5567 (2006).
15. M. Chami, "Importance of the polarization in the retrieval of oceanic constituents from the remote sensing reflectance," J. Geophys. Res. **112**(2007).
16. J. L. Deuze, M. Herman, and R. Santer, "Fourier-series expansion of the transfer equation in the atmosphere ocean system," J. Quant. Spectrosc. Radiat. Transfer **41**, 483-494 (1989).
17. G. G. Stokes, Trans. Cambridge Philos. Soc. **3,** (1852).
18. Y. Kawata, A. Yamazaki, T. Kusaka, and S. Ueno, "Aerosol retrieval from airborne Polder data by multiple scattering model," in *Geosci. Remote Sens. Symp., 1994. IGARSS '94. Surface and Atmospheric Remote Sensing: Technologies, Data Analysis and Interpretation., International*, (1994), 1895-1897.
19. E. P. Shettle and R. W. Fenn, "Models for the aerosols of the lower atmosphere and the effect of humidity variations on their optical properties," in *Environmental Research Paper Air Force Geophysics Lab., Hanscom AFB, MA. Optical Physics Div.*, P. Tsipouras and H. B. Garrett, eds., (1979).
20. H. R. Gordon and M. Wang, "Retrieval of water leaving radiance and aerosol optical thickness over the oceans with seawifs: a preliminary algorithm," Appl. Opt. **33**, 443-458 (1994).
21. M. H. Wang, K. D. Knobelspiesse, and C. R. McClain, "Study of the Sea-Viewing Wide Field-of-View Sensor (SeaWiFS) aerosol optical property data over ocean in combination with the ocean color products," J. Geophys. Res. **110,** D10S06, doi:10.1029/2004JD004950 (2005).
22. C. R. McClain, G. C. Feldman, and S. B. Hooker, "An overview of the SeaWiFS project and strategies for producing a climate research quality global ocean bio-optical time series," Deep-Sea Research Part II-Topical Studies In Oceanography **51**, 5-42 (2004).
23. A. Morel, *Optical Properties of Pure Water and Pure Seawater, in Optical Aspects of Oceanography*, (Academic Press, New York, 1974), pp. 1-24.
24. R. M. Pope and E. S. Fry, "Absorption spectrum (380-700 nm) of pure water. II. Integrating cavity measurements," Appl. Opt. **36**, 8710-8723 (1997).
25. A. Bricaud, A. Morel, M. Babin, K. Allali, and H. Claustre, "Variations of light absorption by suspended particles with chlorophyll a concentrationin oceanic (case 1) waters: analysis and implications for bio-optical models," J. Geophys. Res. **103**, 31033 (1998).
26. H. Loisel and A. Morel, "Light scattering and chlorophyll concentration in case 1 waters: A reexamination," Limnol. Oceanogr. **43**, 847-858 (1998).
27. H. Bader, "Hyperbolic distribution of particle sizes," J. Geophys. Res. **75**, 2822-& (1970).
28. D. Stramski, E. Boss, D. Bogucki, and K. J. Voss, "The role of seawater constituents in light backscattering in the ocean," Progress in Oceanography **61**, 27-56 (2004).
29. A. C. Holland and G. Gagne, "Scattering of polarized light by Polydisperse Systems of irregular particles," Appl. Opt. **9**, 1113-1121 (1970).
30. G. N. Plass and G. W. Kattawar, "Radiance and Polarization of Earths Atmosphere with Haze and Clouds," J. Atmos. Sci. **28**, 1187-1198 (1971).

#91057 - $15.00 USD Received 20 Dec 2007; revised 6 Feb 2008; accepted 13 Feb 2008; published 15 Apr 2008

31. E. S. Fry and K. J. Voss, "Measurement of the Mueller Matrix for Phytoplankton," Limnol. Oceanogr. **30**, 1322-1326 (1985).
32. K. J. Voss and E. S. Fry, "Measurement of the Mueller Matrix for Ocean Water," Appl. Opt. **23**, 4427-4439 (1984).
33. D. Stramski, A. Bricaud, and A. Morel, "Modeling the inherent optical properties of the ocean based on the detailed composition of the planktonic community," Appl. Opt. **40**, 2929-2945 (2001).
34. A. Morel, B. Gentili, H. Claustre, M. Babin, A. Bricaud, J. Ras, and F. Tieche, "Optical properties of the "clearest" natural waters," Limnol. Oceanogr. **52**, 217-229 (2007).
35. J. L. Deuze, P. Goloub, M. Herman, A. Marchand, G. Perry, S. Susana, and D. Tanre, "Estimate of the aerosol properties over the ocean with POLDER," J. Geophys. Res. **105**, 15329-15346 (2000).
36. D. Antoine and A. Morel, "Oceanic primary production 1. Adaptation of a spectral light-photosynthesis model in view of application to satellite chlorophyll observations," Global Biogeochem. Cycles **10**, 43-55 (1996).
37. F. Waquet, J. F. Leon, P. Goloub, J. Pelon, D. Tanre, and J. L. Deuze, "Maritime and dust aerosol retrieval from polarized and multispectral active and passive sensors," J. Geophys. Res. **110**(2005).
38. D. Antoine and A. Morel, "A multiple scattering algorithm for atmospheric correction of remotely sensed ocean colour (MERIS instrument): principle and implementation for atmospheres carrying various aerosols including absorbing ones," Int. J. Remote Sens. **20**, 1875-1916 (1999).
39. H. Fukushima, A. Higurashi, Y. Mitomi, T. Nakajima, T. Noguchi, T. Tanaka, and M. Toratani, "Correction of atmospheric effects on ADEOS/OCTS ocean color data: algorithm description and evaluation of its performance," J. Oceanogr. **54**, 417-430 (1998).
40. D. Antoine, M. Chami, H. Claustre, F. d'Ortenzio, A. Morel, G. Bécu, B. Gentili, F. Louis, J. Ras, E. Roussier, A. Scott, D. Tailliez, S. B. Hooker, P. Guevel, J. F. Desté, and D. Adams, "BOUSSOLE: A Joint CNRS-INSU, ESA, CNES and NASA Ocean Color Calibration and Validation Activity," (NASA, 2006).
41. F. S. Zhao, Z. B. Gong, H. L. Hu, M. Tanaka, and T. Hayasaka, "Simultaneous determination of the aerosol complex index of refraction and size distribution from scattering measurements of polarized light," Appl. Opt. **36**, 7992-8001 (1997).

1. Introduction

PARASOL (Polarization and Anisotropy of Reflectance for Atmospheric Sciences coupled with Observations from a Lidar) satellite instrument has recently been deployed (in 2005) to provide complete observations of radiative properties of the earth's atmosphere and ocean. The PARASOL sensor, which is a heritage of POLDER instruments [1], is unique inasmuch as it is currently the only one that is capable of performing multiangular and polarized acquisitions from space combined with the spectral information. The PARASOL instrument monitors the intensity (i.e. Stokes parameters *I*) of sunlight exiting the terrestrial systems for 9 spectral bands in the range 443-1020 nm and for up to 16 viewing angles. In addition, PARASOL measures the linearly polarized components (i.e., Stokes parameters *Q* and *U*) of upward radiation for three spectral bands, namely 490 nm, 670 nm and 865 nm. Both the total and polarized radiance measured by PARASOL exhibit dependencies on scattering angle and wavelength that can be used to extract information from the atmosphere and ocean. Polarization state of light is a piece of information that is complementary to the spectral and angular radiance measurements. It has been shown that polarization of the atmospheric radiation is more sensitive to microphysical properties of aerosols than the unpolarized radiance is [2-4]. Therefore, many studies have been dedicated to the characterization of aerosols using either ground-based or satellite/airborne measurements of atmosphere polarization [5-9]. Ground-based measurements could be not only used in near-infrared channels [5, 9] but also in visible bands [6] because such measurements are not affected by surface effects. On the other hand, the exploitation of satellite or airborne remotely sensed data is currently limited to the use of red/near infrared wavelengths [8] because of the lack of knowledge of the magnitude of polarized water leaving radiance [7]. As a result and despite the excellent performances of the PARASOL system [10, 11], PARASOL polarized measurements acquired at short wavelengths have not been exploited yet to derive information on aerosol properties for ocean color purposes such as the derivation of unpolarized water leaving radiances from space. Recent studies [12-15] showed that the polarized contribution of the underwater light field is negligibly small relatively to that of the atmosphere and air-water interface in the visible spectral range for most open ocean waters. Therefore, the range of wavelengths used for aerosol retrieval over the open oceans could be

#91057 - $15.00 USD Received 20 Dec 2007; revised 6 Feb 2008; accepted 13 Feb 2008; published 15 Apr 2008

expanded in the visible part of the spectrum. More specifically, Chami [15] suggested in a preliminary study that multiangle measurements of polarized radiance at blue wavelengths could be potentially exploited to obtain additional valuable information of the spectral behavior of aerosol optical properties. On this basis, the performance of atmospheric correction algorithms could be improved over the global ocean and a better retrieval of unpolarized water leaving radiances could be expected from satellite polarized data acquired in the visible bands. However, the simulations performed in Chami's paper [15] were restricted to the solar principal plane and thus, they could not practically apply to satellite images for which targets are observed for azimuth geometries that can be far from principal plane conditions.

It is the purpose of this paper to examine whether the invariance properties of top of atmosphere polarized signal with water content could be expanded for all geometries that can be found in ocean colour satellite sensors measurements. Our analysis focuses particularly on PARASOL viewing geometries and radiometric specifications (i.e., instrumental noise) to determine the degree of applicability of Chami's theoretical results [15] in the case of real world conditions. Another goal of this paper is to perform a rigorous validation of theory using PARASOL measurements acquired over open ocean waters. Note that it is the first time, to our knowledge, that the specificities of PARASOL images are exploited for ocean color remote sensing purposes. This study also highlights the relevance of the concept of multidirectionality which allows extending the set of remote sensing information available for deriving aerosol optical properties.

This paper is organized as follows. First, radiative transfer calculations are carried out to characterize the influence of water content on the polarized signal at the top of atmosphere in the visible band (490 nm) for different atmospheric conditions and for an exhaustive set of geometries. Second, the potential applicability of these calculations is evaluated using a representative set of PARASOL geometrical conditions derived from measurements acquired in different parts of the globe. Finally, a validation of theoretical results is carried out based on PARASOL satellite data measured at regional (e.g., Mediterranean Sea) and global (e.g. Atlantic Ocean) scales.

2. Theoretical analysis

2.1 Radiative transfer simulations

Top of atmosphere (TOA) polarized reflectances were calculated for various atmospheric, oceanic and geometrical conditions using the OSOA radiative transfer model [12]. The OSOA model solves the vector radiative transfer equation for the atmosphere-ocean system using the successive orders of scattering method [16]. For a given solar angle θ_s, the Stokes parameters *I*, *Q* and *U*, which characterize the intensity, the degree of polarization and the direction of polarization of the electromagnetic wave respectively [17], are computed for viewing angles θ_v ranging from 0° to 90° and azimuth ϕ ranging from 0° to 180°. The OSOA model considers a flat ocean surface. Therefore, the influence of the wind on the surface is not taken into account in this study and thus, the results that will be presented may be less general. However, it has been shown that the effect of the waves on the polarized signal measured at the top of atmosphere level from space is weak [18]. Based on Kawata, *et al.'s* analysis [18], the fact that the wind effect is not accounted for in the OSOA model may not drastically affect our results with regard to the interpretation of the variations in the polarized TOA signal with atmospheric and oceanic constituents. The atmospheric layer was modelled using realistic aerosol models namely the standard maritime M98 and tropospheric T70 as defined by Shettle and Fenn [19]. The M98 and T70 models were selected because they exhibit significant differences in their optical thickness spectral dependence (i.e., fairly neutral spectral shape for M98 and strong decrease with wavelength for T70) [20, 21]. Note that despite their strong differences, the M98 and T70 models are not the models that show the largest spectral variations of the aerosol models that are currently used in SeaWiFS and MODIS data processing [21, 22]. The computations were carried out for two values of the aerosol optical

#91057 - $15.00 USD Received 20 Dec 2007; revised 6 Feb 2008; accepted 13 Feb 2008; published 15 Apr 2008

depth τ_a at 550 nm, namely 0.1 and 0.5, which are representative of the range of variation typically found over open ocean waters. Note that these values of τ_a at 550 nm correspond to horizontal visibilities of 50 km and 8 km respectively. At 490 nm, the values of τ_a, for each of the visibilities, are 0.1 and 0.5 for M98 model and 0.12 and 0.61 for T70 model. In the OSOA model, the oceanic layer is usually described using a seawater model comprising four components which are pure seawater, phytoplankton pigments and their by-products, inorganic suspended material and colored dissolved organic matter. Since this study focuses on the analysis of signal variations over phytoplankton-dominated water type, only the pure seawater and phytoplankton components were considered here. The inherent optical properties of these components were modelled as follows. The scattering and absorption coefficients of pure seawater were taken from Morel [23] and Pope and Fry [24] respectively. The absorption coefficient of phytoplankton and co-varying particles a_{ph} was derived by use of the bio-optical model of Bricaud, *et al.* [25] [Eq. (1)] :

$$a_{ph}(\lambda)=A_{ph}(\lambda)[Chl]^{Ep(\lambda)} \tag{1}$$

where *Chl* is the chlorophyll *a* concentration (in mg m^{-3}), $A_{ph}(\lambda)$ and $E_p(\lambda)$ are tabulated coefficients. The phytoplankton scattering coefficient was modelled as suggested by Loisel and Morel [26] [Eq. (2)] :

$$b_{ph}(\lambda)=0.416[Chl]^{0.766}\left(\frac{550}{\lambda}\right) \tag{2}$$

The refractive index of phytoplankton relative to water was 1.05. The size distribution of phytoplankton cells was assumed to follow the Junge hyperbolic function, which is often used for natural waters [27], with a Junge exponent value of –4. The minimum and maximum radii of the size distribution were 0.1 µm and 50 µm respectively. The Mueller scattering matrix of phytoplankton, which contains the information on its total and polarized phase function, was computed by means of Mie theory [28]. It has been argued that reasonable fits to the phase function (first term of the Mueller scattering matrix) can be obtained using Mie theory [29-33]. The normalised polarized phase function of phytoplankton (i.e., the polarized phase function divided by the unpolarized phase function), which is calculated here using realistic parameters for phytoplankton, is very close to the Rayleigh approximation. Therefore, the simulated polarization features of phytoplankton are in agreement with what has been found for natural ocean water samples [32] and thus, making our computations meaningful.

The OSOA model outputs the angular distribution of the polarized reflectance ρ_{pol} [Eq. (3)] at the top of atmosphere level:

$$\rho_{pol}=\frac{\pi\sqrt{Q^2+U^2}}{E_d} \tag{3}$$

In Eq. (3), E_d is the downwelling irradiance (in W m^{-2}) and $\sqrt{Q^2+U^2}$ is the polarized radiance. The computations were carried out for solar zenith angles θ_s varying from 0° to 70°, for azimuth angles varying from 0° to 180° and for viewing angles varying from 0° to 90°. The angular resolution was 5° when dealing with θ_s and ϕ and 2° when dealing with θ_v. The polarized reflectance was analyzed at 490 nm, which is consistent with the PARASOL polarized visible band. The concentrations of chlorophyll *a* used in the calculations were 0.03, 0.1, 0.3, 0.5, 1, 3 and 10 mg m^{-3}.

#91057 - $15.00 USD Received 20 Dec 2007; revised 6 Feb 2008; accepted 13 Feb 2008; published 15 Apr 2008

2.2 Results and discussion

The influence of phytoplankton particles on the TOA polarized reflectance is theoretically studied for various geometries. The contribution from atmospheric molecules to the polarized TOA reflectance, which was calculated using Rayleigh theory, has been subtracted for each Stokes parameter to emphasize the polarized signature of aerosols and/or hydrosols. The polarized reflectance obtained after subtracting the atmospheric molecules effects is called the Rayleigh-corrected polarized reflectance in the rest of the paper. To evaluate the sensitivity of the Rayleigh-corrected polarized reflectance, hereafter referred to as ρ_{pol_rc}, with the turbidity of the water mass, the absolute difference $\Delta\rho_{pol\_rc}$ between the Rayleigh-corrected polarized reflectance calculated for a given chlorophyll *a* concentration and the Rayleigh-corrected polarized reflectance calculated for a chlorophyll *a* concentration taken as a reference is analysed according to Eq. (4):

$$\Delta\rho_{pol\_rc}(Chl) = \left|\rho_{pol\_rc}(Chl) - \rho_{pol\_rc}(Chl_{ref})\right| \quad (4)$$

where *Chl* is a given chlorophyll *a* concentration and Chl_{ref} is the chlorophyll *a* concentration taken as a reference, which represents the residual content for open ocean, namely 0.03 mg m^{-3} [34].

2.2.1 Variations of the TOA polarized reflectance with water turbidity

The first case considered is the variation in ρ_{pol_rc} with phytoplankton concentrations for all viewing geometries. Figure 1 shows polar diagrams of $\Delta\rho_{pol\_rc}(Chl)$ at 490 nm for θ_s=30° and 50° and for various chlorophyll *a* concentrations. The simulations were carried out for a clear (i.e., τ_a(550 nm) = 0.1, Fig. 1) and a moderately turbid atmosphere (i.e., τ_a(550 nm) = 0.5, Fig. 2) using the M98 aerosol model. The azimuth angle shown in Fig. 1 and other forthcoming similar figures corresponds to the azimuth difference between the solar and observation plane. As an example, an azimuth difference of 0° means that the half planes containing the sun and the sensor are similar while an azimuth difference of 180° means that the sun and the sensor are located in two opposite planes. For a clear atmosphere (Fig. 1), the absolute difference $\Delta\rho_{pol\_rc}(Chl)$ is lower than 8×10^{-4} whatever the observation geometry and solar zenith angle when chlorophyll *a* concentrations are smaller than 1 mg m^{-3}. The influence of marine particles on ρ_{pol_rc} increases with their concentration and is dependent on the observation geometry. As an example, the principal impact of the marine particles, when the value of chlorophyll *a* concentration and θ_s is 3.0 mg m^{-3} and 30° respectively, is limited to the range of azimuth angles 120°-180°. Note that these observation geometries are often sun glint contaminated [35], and thus, they are not necessarily exploited for remote sensing studies over the ocean. The influence of water content on TOA signal is reduced for higher solar zenith angle (e.g., θ_s=50°). This is because the atmospheric pathlength of the radiation is longer in this latter case and the impact of the atmosphere increases, thus reducing significantly the effect of the hydrosols signature. For similar reasons, the variations in ρ_{pol_rc} with the chlorophyll *a* concentration observed in the azimuth range 120°-180° decrease as the atmosphere gets more turbid (Fig. 2). The variations remain smaller than 8×10^{-4} whatever the viewing geometries when the aerosol optical depth is 0.5. This latter result confirms the prevailing effect of aerosols on the polarization in comparison to the phytoplankton content of the oceanic layer. The computations made using the T70 aerosol model showed similar features as those obtained for the M98 aerosol model.

#91057 - $15.00 USD Received 20 Dec 2007; revised 6 Feb 2008; accepted 13 Feb 2008; published 15 Apr 2008

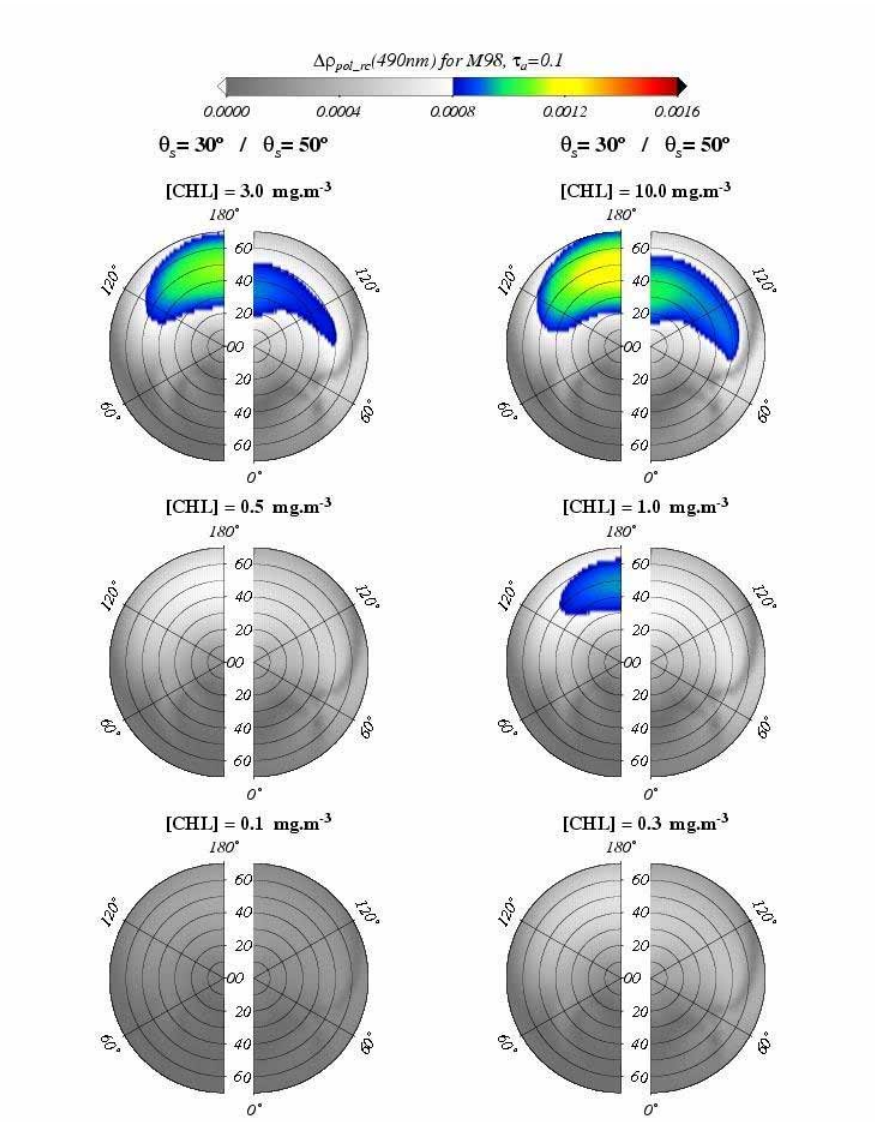

Fig. 1. Polar diagrams of absolute difference $\Delta\rho_{pol\_rc}$ between the Rayleigh-corrected polarized reflectance calculated for any given chlorophyll *a* concentration and the one calculated for a chlorophyll *a* concentration of 0.03 mg m^{-3}. The circular dot lines represent the viewing angles by step of 10° (numbered from 0° to 60° in the figure). The solar zenith angles θ_s are 30° and 50° and the Shettle and Fenn [19] aerosol model M98 is used. The calculations are shown for a clear atmosphere ($\tau_a(550)$=0.1). Note that a grey color scale is used when $\Delta\rho_{pol\_rc}$ is lower than PARASOL noise equivalent polarized reflectance (i.e., 8.5×10^{-4}).

Fougnie, *et al*., [10] recently showed based on an in-flight calibration study that the noise equivalent polarized reflectance of PARASOL sensor at 490 nm is 8.5×10^{-4} for ocean targets, which is consistent with preflight estimation and specification of the instrument. Therefore, from an instrumental viewpoint, the polarized reflectance at the top of atmosphere is practically not sensitive to optically active marine particles in the case of a turbid atmosphere (Fig. 2). In the case of a clear atmosphere, similar conclusions can be drawn only for waters showing *Chl* concentrations lower than 1 mg m^{-3} (Fig. 1), which represent more than 90% of global ocean waters [36]. As reported by Chami [15], the contribution to TOA polarized reflectance is predominantly from the atmospheric particles and, to a lesser extent, the

#91057 - $15.00 USD Received 20 Dec 2007; revised 6 Feb 2008; accepted 13 Feb 2008; published 15 Apr 2008

skylight Fresnel reflection at the sea surface which both significantly reduce the already weak polarization effects induced by biogenic marine particles [12]. It should be highlighted that one significant difference between previous studies [13-15] and the current one is that, here, the polarized reflectance has been corrected for atmospheric molecular effects to emphasize the role played by the aerosols. Our results show that the sole aerosol polarized signature is sufficiently appreciable, including in the case of a clear atmosphere, to mask the influence of the hydrosols on the TOA polarized signal, despite the strong influence of the atmospheric molecular scattering on the polarization features.

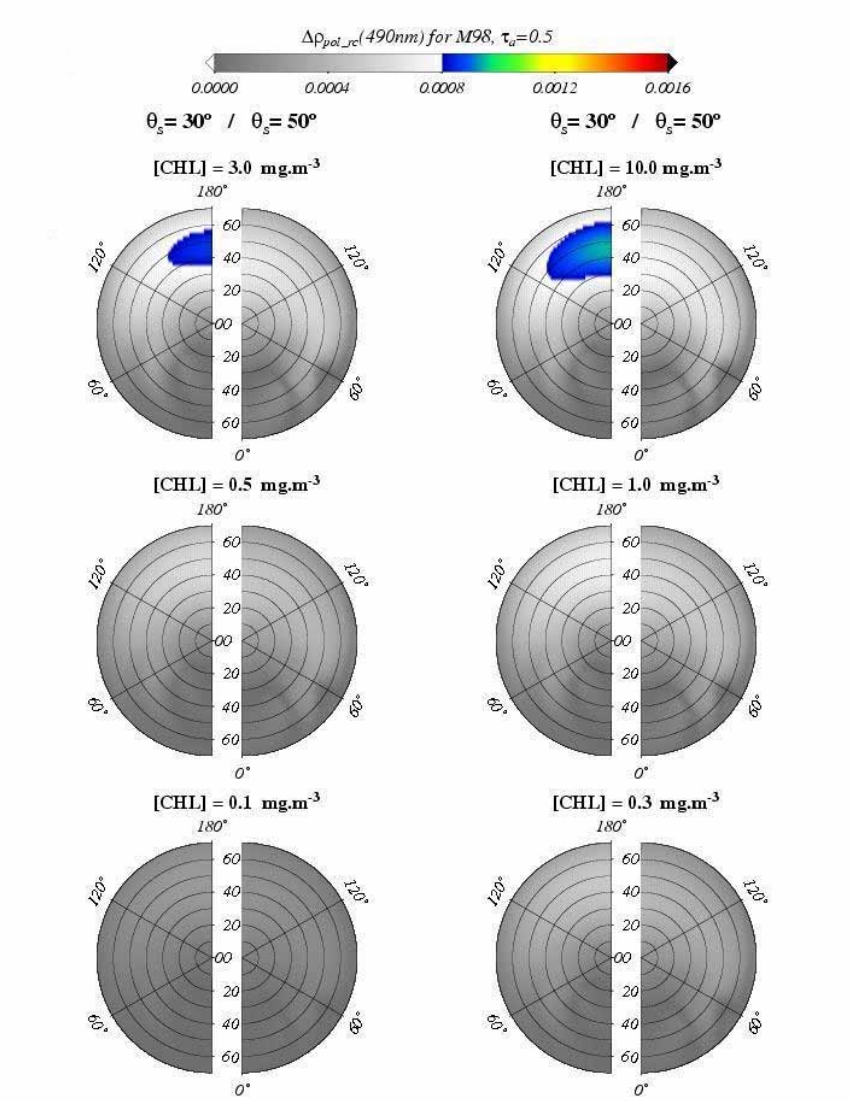

Fig. 2. Same as Fig. 1, for a moderately turbid atmosphere (τ_a(550)=0.5).

To quantify the aerosol polarization signature, the sensitivity of ρ_{pol_rc} at TOA to the aerosol model was studied for clear (Fig. 3, first column) and moderately turbid (Fig. 3, second column) atmospheres. The polar diagrams shown in Fig. 3 represent the absolute difference $\Delta\rho_{pol\_aero\_mod}$ between ρ_{pol_rc} calculated using the M98 model and ρ_{pol_rc} calculated for two other standard aerosol models, namely the C70 and T70 models. The chlorophyll *a* concentration was fixed to 0.3 mg m^{-3} and $\Delta\rho_{pol\_aero\_mod}$ is displayed for solar zenith angles values of 30° and 50°. Note that the value of the chlorophyll *a* concentration is not critical

#91057 - $15.00 USD Received 20 Dec 2007; revised 6 Feb 2008; accepted 13 Feb 2008; published 15 Apr 2008

here because of the negligible influence of the marine polarized signal. Significant variations of $\Delta\rho_{pol\_aero\_mod}$ are observed with respect to the geometrical conditions for the two cases of atmospheric turbidity. The polarization features induced by aerosols which show significant differences in their optical properties, such as their spectral variation, are distinguishable (i.e., greater than the instrumental noise) for the majority of the observation geometries. Therefore, in addition to their optical depth, the polarizing and directional properties of aerosols could be extracted at visible wavelengths over open ocean waters. Even though some geometries show a value of $\Delta\rho_{pol\_aero\_mod}$ lower than PARASOL noise equivalent polarized reflectance, they can still be exploited to derive information on the aerosol optical properties from satellite multiangle measurements by comparing those pixels with pixels originating from the same target and for which a significant variation of $\Delta\rho_{pol\_aero\_mod}$ is observed. Note that the latter comparison can systematically be applied on PARASOL scenes owing to the multidirectional principle of acquisition of PARASOL images.

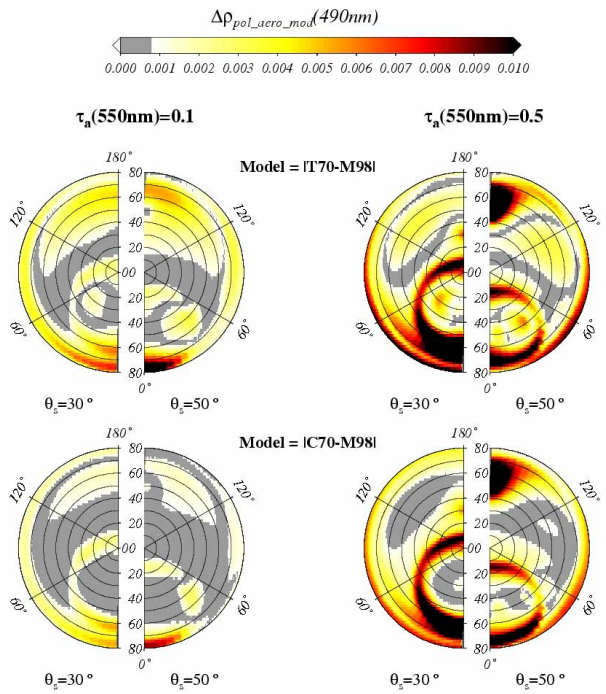

Fig. 3. Polar diagrams of the absolute differences between the Rayleigh-corrected polarized reflectance calculated for the M98 aerosol model taken as a reference and the Rayleigh-corrected polarized reflectance calculated for the aerosol models C70 and T70, respectively. The chlorophyll *a* concentration is fixed to 0.3 mg m^{-3}, the solar zenith angles are 30° and 50° for a clear atmosphere (τ_a(550nm)=0.1) (first column), and a turbid atmosphere (τ_a(550nm)=0.5) (second column). The geometries for which $\Delta\rho_{pol\_rc}$ is lower than PARASOL noise equivalent polarized reflectance (i.e., 8.5×10^{-4}) are in coloured grey.

3. Validation of theoretical results using PARASOL measurements

The main originality of PARASOL instrument is its capacity to characterize the directional and polarization effects of a given target from space. The innovative concept of this instrument allowed various aerosols studies over the ocean [8, 35, 37]. Note that these studies did not account for the directional and polarized measurements in the visible band because of the uncertainty in the polarized water leaving radiance. It has been demonstrated that a high performance of atmospheric correction algorithms in visible channels is required to accurately determine ocean color geophysical products such as chlorophyll *a* concentration [20, 38, 39].

#91057 - $15.00 USD Received 20 Dec 2007; revised 6 Feb 2008; accepted 13 Feb 2008; published 15 Apr 2008

In this prospect and based on our theoretical results, the use of PARASOL polarized measurements in the visible band seems promising for improving the remote sensing of aerosols and thus, for retrieving ocean color parameters. In this section, the degree of applicability of the previous theoretical results (see section 2.2) to PARASOL images is investigated. Our first objective is to focus on the orbitography of PARASOL satellite to identify the number of geometrical observations conditions for which ρ_{pol_rc} is theoretically invariant with phytoplankton concentration. Our second objective is to validate the property of invariance of the top of atmosphere multidirectional polarized reflectance acquired in visible spectral bands with water turbidity using PARASOL measurements.

3.1 Applicability of theory to PARASOL images

PARASOL images acquired along two satellite overpasses in the latitude range 70°N-70°S were processed. The values of the longitude at the equator of both PARASOL satellite strips were centered around 150°W and 30°W to include the Pacific Ocean [Fig. 4(a)] and Atlantic Ocean [Fig. 4(b)] and thus, covering the majority of the geometrical observations made by the PARASOL instrument over the global ocean. Based on the geometrical conditions of observation of a given target viewed by PARASOL (i.e., azimuth and viewing angles), the absolute difference $\Delta\rho_{pol\_rc}(Chl=3.0\ \text{mg m}^{-3})$ was calculated in the case of a clear atmosphere ($\tau_a=0.1$) using the aerosol model M98 (see Fig. 1). Note that such a turbidity corresponds to the case for which the influence of marine constituents is the greatest relatively to higher values of the turbidity (see Fig. 1 and Fig. 2). If $\Delta\rho_{pol\_rc}$ is lower than the noise equivalent polarized reflectance of PARASOL, the property of insensitivity of the TOA polarized signal to the phytoplankton concentration is attributed to the viewed target. The results show that 87% (table 1) of the targets are viewed by PARASOL under geometries for which the top of atmosphere polarized reflectance is not sensitive to the oceanic turbidity. This means that PARASOL polarized measurements in the visible band are practically exploitable exclusively for deriving information upon atmospheric particles for 87% of the targets observed within a PARASOL image. Note that the value of this proportion reaches 95% for targets located within the latitude range 60°N-60°S. Similar results were obtained when the simulations were carried out using T70 aerosol model, thus indicating that the marine polarized signature is too weak to influence the atmospheric effects on the TOA polarized reflectance. Note that the results shown in table 1 were derived for extreme conditions inasmuch as values of phytoplankton concentration greater than 3.0 mg m^{-3} only represent less than 5 % of the cases found in the global ocean [36]. Based on Figs. 1 and 2, TOA polarized reflectance at 490 nm could be examined and analysed regardless of the contribution of subsurface suspended matter in almost any case when dealing with open ocean waters showing a chlorophyll *a* concentration lower than 3.0 mg m^{-3}. Therefore, the theoretical sensitivity study performed in section 2 is largely applicable (i.e., for a great majority of the open ocean waters) to PARASOL instrument from an operational viewpoint.

The property of invariance of ρ_{pol_rc}(TOA) with water turbidity is now tested and validated using PARASOL measurements. First, the test was carried out for images acquired above a given relevant site (i.e., regional scale) for which derived geophysical products such as chlorophyll *a* concentration or atmospheric parameters were available. Second, a more global analysis was performed based on satellite overpasses covering the latitude range 60°N-60°S (i.e., global scale).

#91057 - $15.00 USD Received 20 Dec 2007; revised 6 Feb 2008; accepted 13 Feb 2008; published 15 Apr 2008

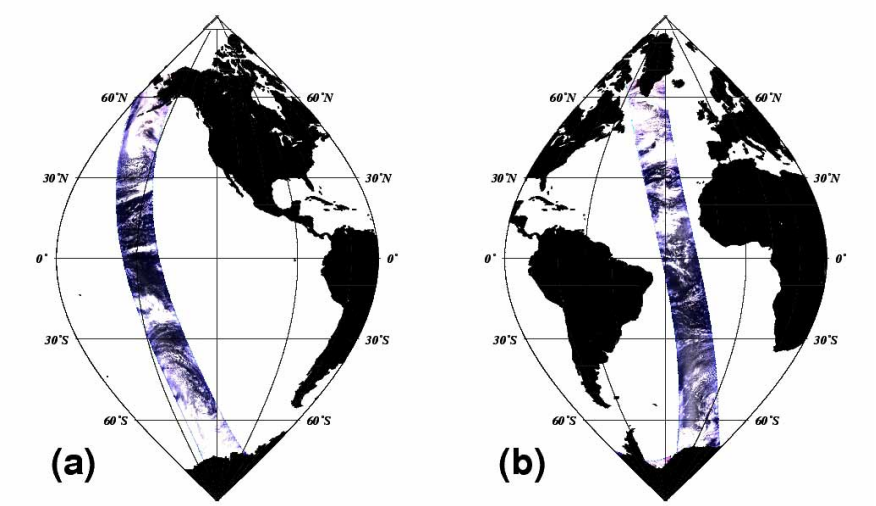

Fig. 4. PARASOL satellite overpasses used for the statistical analysis regarding the geometrical conditions of observations (a) above the Pacific Ocean (the longitude at the equator is 150°W), and (b) above the Atlantic Ocean (the longitude at the equator is 30°W). The latitude varies from 70°N to 70°S.

Table 1. Percentage of targets viewed by PARASOL for which the polarized top of atmosphere reflectance is insensitive to chlorophyll *a* concentration along two satellite overpasses covering the Atlantic Ocean and Pacific Ocean. The longitudes at the equator of satellite overpasses above the Atlantic and Pacific oceans are 30°W and 150°W respectively.

	Overpass above the Atlantic Ocean	Overpass above the Pacific Ocean
Percentage when targets are located between 70°N and 70°S	87.8%	87.8%
Percentage when targets are located between 60°N and 60°S	94.8%	94.9%

3.2 Validation of theory using PARASOL data

3.2.1 Validation at regional scale

To achieve the validation of theory using measurements obtained at a regional scale, satellite scenes acquired above the north western part of the Mediterranean Sea, which is considered as open ocean water type [40], were studied. PARASOL level 2 geophysical products were used to get information on aerosol and oceanic optical properties. Note that the level 1 (i.e. calibrated data) and level 2 (i.e., geophysical parameters) atmospheric products were provided by the ICARE organization (http://www-icare.univ-lille1.fr/main.php) and the level 2 ocean color products (i.e. *Chl*) were provided by HYGEOS company (http://web.hygeos.com). The analysis was carried out for images acquired during the spring bloom, in May 2006, which showed a significant gradient of chlorophyll *a* concentrations. To evaluate the sole effect of the subsurface suspended particle on the polarized reflectance measured at TOA, two targets showing homogenous aerosol optical properties and a significant variation in chlorophyll *a* concentrations were selected. The atmosphere could be considered as homogenous when both the atmospheric turbidity and the aerosol spectral properties are similar for each target. Therefore, targets exhibiting identical values of aerosol optical thickness at 865 nm (within

#91057 - $15.00 USD Received 20 Dec 2007; revised 6 Feb 2008; accepted 13 Feb 2008; published 15 Apr 2008

±0.01) and identical values of the Angstrom coefficient (within ±0.1), which characterizes the spectral variation of aerosols, were selected [Figs. 5(a) and 5(b)]. The values of the aerosol optical depth at 865 nm and the Angstrom coefficient were 0.10 and 1.2 respectively for the selected targets, thus inducing a value of the aerosol optical depth of 0.15 at 490 nm. The chlorophyll *a* concentrations varied from 0.2 mg m^{-3} to 2 mg m^{-3} for the target located out of the bloom and within the bloom patch respectively [Fig. 5(c)]. The coordinates of the target located out of the bloom and within the bloom patch are (42.15°N, 6.35°E) and (40.07°N, 6.50°E) respectively. Note that the geophysical products derived from PARASOL were highly consistent with SeaWiFS level 2 products in the same area. In particular, similar gradients of chlorophyll *a* concentrations and homogeneity of aerosol optical properties were observed for both satellite sensors. It should be highlighted that the exact absolute values of atmospheric and oceanic parameters provided by level 2 satellite products are not of great interest for the purpose of this study. Level 2 satellite geophysical products are just used here qualitatively to inform us about the relative spatial variations or spatial homogeneities of environmental parameters (i.e. chlorophyll *a*, optical depth, Angstrom coefficient) between two targets.

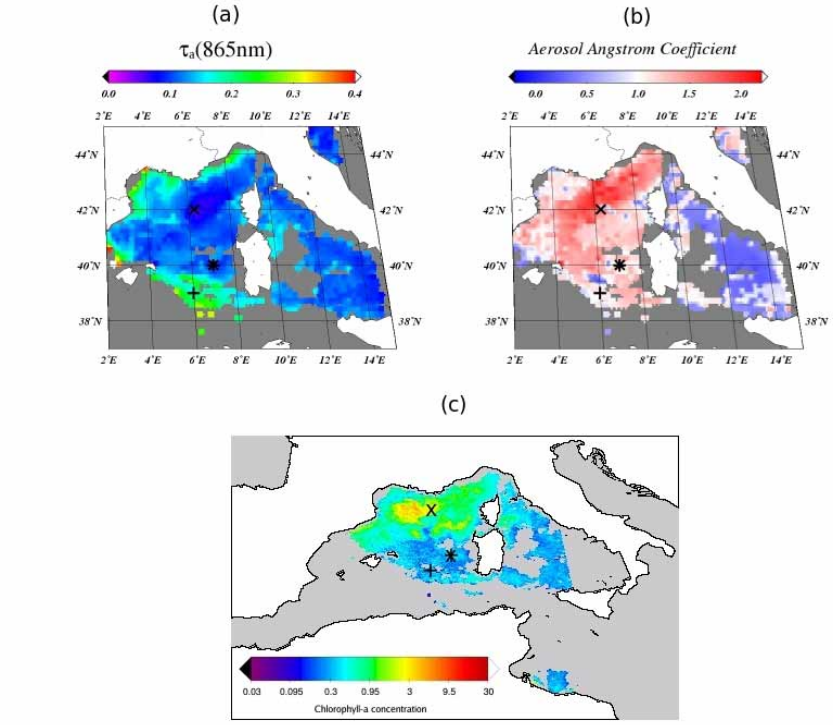

Fig. 5. Level 2 satellite images acquired by PARASOL above the North Western part of the Mediterranean Sea on May 5th 2006: (a) aerosol optical depth at 865 nm, (b) Angstrom coefficient and (c) chlorophyll *a* concentration. Three targets were selected : one target (symbol *) is characterized by a clear atmosphere (τ_a(865nm)=0.1) and oligotrophic conditions (*Chl*=0.2 mg m^{-3}), one target (symbol ×) is characterized with similar atmospheric conditions than the target represented by the symbol * except bloom conditions (*Chl*=2.0 mg m^{-3}) are considered, and one target (symbol +) is characterized by a moderately turbid atmosphere (τ_a(865nm)=0.3) and similar oceanic conditions (*Chl*=0.2 mg m^{-3}) than the target represented by the symbol *.

Figure 6(a) shows the angular variations in the TOA Rayleigh-corrected polarized reflectance at 490 nm, as obtained from level 1 PARASOL data, for the targets located within and outside the bloom patch (symbols * and × in Fig. 5). The polar diagram [Fig. 6(b)] shows that both targets are viewed under close geometrical conditions, as expected from the fact that the longitudes of the targets are quite similar. The comparison between $\rho_{pol\_rc}(TOA)$ measured

#91057 - $15.00 USD Received 20 Dec 2007; revised 6 Feb 2008; accepted 13 Feb 2008; published 15 Apr 2008

for both situations shows a good agreement. The root mean square error (RMSE), which is defined as Eq. (5), was calculated to quantify the absolute differences between the measurements obtained within and outside the bloom area.

$$RMSE = \sqrt{\frac{1}{n}\sum_{i=1}^{n}(\rho_{pol\_rc}(bloom, \boldsymbol{\Psi}_i) - \rho_{pol\_rc}(no\_bloom, \boldsymbol{\Psi}_i))^2} \quad (5)$$

In Eq. (5), $\boldsymbol{\Psi}_i$ is the vector representing the observation geometry which accounts for the azimuth, the solar zenith angle and the viewing zenith angle and *n* is the number of directions of observations which was 14 here. Interestingly, the value of the *RMSE* is 6.2×10^{-4} which remains lower than the instrumental noise of PARASOL sensor. As a comparison, Fig. 6 also reports the results obtained when the unpolarized reflectance is considered. The *RMSE* value in this latter case, namely 6.7×10^{-3}, is greater by more than one order of magnitude than the sensitivity of PARASOL instrument, which is 4×10^{-4} for unpolarized measurements. One can think that the differences observed between the *RMSE* calculated for the unpolarized reflectance and the *RMSE* calculated for the polarized reflectance could be exclusively due to the fact that the unpolarized measurements are usually one order of magnitude greater than the polarized reflectance. To verify that these differences are not necessarily attributed to magnitude differences in the TOA polarized and unpolarized reflectances, the contribution from instrumental noise and phytoplankton concentration to the variations observed in the reflectance between the oligotrophic and blooming conditions is examined. To achieve such a task, a statistical analysis based on the chi-square test was performed. The following hypothesis was tested: "all the variations observed in the reflectance between the oligotrophic and blooming conditions are due exclusively to the instrumental noise in the measurements". The results of the test indicated that the hypothesis is totally rejected when dealing with the unpolarized reflectance, thus confirming that the variations observed in Fig. 6(a) (top curves) are attributed to variations in the phytoplankton concentration and not to the instrumental noise. Conversely, the results of the chi-square test point out that the variations observed in the polarized reflectances between the oligotrophic and blooming conditions [Fig. 6(a), bottom curves] are explained by the instrumental noise and not by the variations in phytoplankton concentration. The chi-square analysis thus confirms that the *RMSE* values previously obtained are not exclusively related to the magnitude differences in the TOA polarized and unpolarized reflectance. Based on our statistical analysis (i.e., *RMSE* and chi-square test), the conclusion that can be drawn is that the polarized signal reaching the top of atmosphere in the visible band and measured by PARASOL is practically insensitive to the water turbidity, thus confirming the theoretical results shown in section 2.2 (Fig. 1). It should be highlighted that the invariance of $\rho_{pol\_rc}(TOA)$ with chlorophyll *a* concentration is still observed despite the chlorophyll *a* concentration within the bloom is greater than 1 $mg.m^{-3}$. This is consistent with the fact that the observation geometries of the selected images [see polar diagram of Fig. 6(b)] correspond to theoretical simulated cases for which the invariance property of $\rho_{pol\_rc}(TOA)$ with chlorophyll *a* is verified (see Fig. 1). Those results clearly corroborates that it is not relevant to exploit the polarized signal measured at the top of atmosphere over open ocean waters to extract some information about the optical properties of marine particles. Conversely, as previously suggested by our theoretical calculations (section 2.2), the polarized signal could be used to derive some information about aerosols.

#91057 - $15.00 USD Received 20 Dec 2007; revised 6 Feb 2008; accepted 13 Feb 2008; published 15 Apr 2008

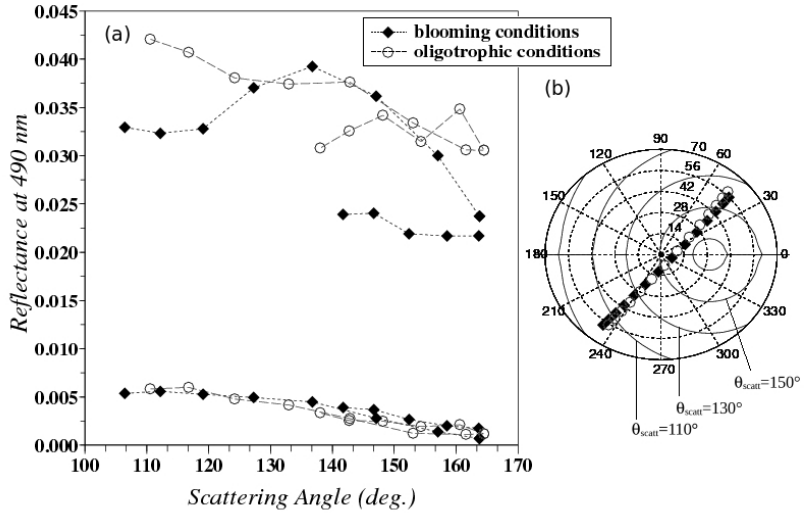

Fig. 6. (a). Variation of the top of atmosphere unpolarized (upper curves) and polarized (lower curves) reflectance measured by PARASOL at 490 nm with respect to the scattering angle θ_{scatt} when the targets are located within the bloom patch (*Chl*=2.0 mg m^{-3}) and out of the bloom patch (i.e., in oligotrophic conditions, *Chl*=0.2 mg m^{-3}) and when the atmospheric conditions are similar for each target, (b) polar diagram showing the geometry of multidirectional observations of the two selected targets. The dashed lines represent the azimuth and viewing angles. The solar zenith angle is 30°. The solid lines represent the isolines of scattering angles by step of 20°. The symbols are similar as in Fig. 6(a).

In this study, the opportunity was given to evaluate the feasibility of deriving information about aerosols using PARASOL measurements. For this purpose, targets showing different aerosol optical properties (optical depth and spectral variation) and identical values of chlorophyll *a* concentration were selected [symbols + and * in Fig. 5(c)] based on the PARASOL level 2 images that were previously analysed. The selected targets show values of τ_a(865 nm) of 0.1 and 0.3, values of Angstrom coefficient of 1.2 and 1.0 respectively and a similar value of *Chl* of 0.2 mg m^{-3}. The coordinates of the atmospherically clear and moderately turbid targets were (40.0°N, 6.9°E) and (38.9°N, 6. 0°E) respectively. Since these targets nearly have a similar longitude, the geometry of multidirectional observations made by PARASOL was almost identical for each target, as shown in the polar diagram of Fig. 7. The angular variations of $\rho_{pol\_rc}(TOA)$ show statistically significant differences between the moderately turbid and the clear atmospheric cases (Fig. 7). First, the differences in the magnitude of the polarized reflectance can be greater than a factor of 2 for specific geometries (i.e., scattering angle lower than 140°). Second, the angular structure of the radiation is highly variable, especially when the atmosphere is turbid. The directional features are more pronounced in the range of scattering angle 120°-150°, which corresponds to the range where the phase function of atmospheric particles is highly dependent on the aerosol optical properties (size and refractive index) [41]. Therefore, Fig. 7 illustrates that the dynamic range of the polarized signal measured at the top of atmosphere, which corresponds to level-1 products of satellite data, is sufficiently high and greater than instrumental noise to make the polarized and angular signatures of aerosols distinguishable and hence, to allow an original characterization of the optical properties of the aerosols. Despite the current study is still a preliminary one, it shows that the radiometric performance of PARASOL satellite instrument is sufficiently accurate in the visible band to significantly improve the aerosol detection over dark target like open ocean waters. The concept of multidirectional and polarization acquisition from space is thus highly promising.

#91057 - $15.00 USD Received 20 Dec 2007; revised 6 Feb 2008; accepted 13 Feb 2008; published 15 Apr 2008

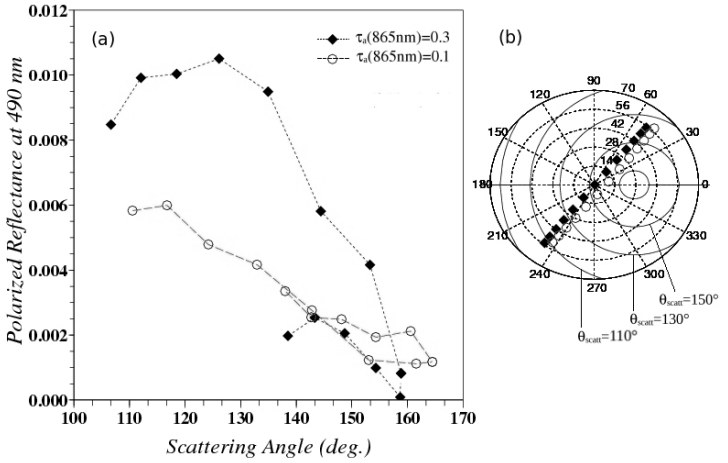

Fig. 7. (a). Variation of the top of atmosphere polarized reflectance measured by PARASOL at 490 nm with respect to the scattering angle θ_{scatt} for targets located outside the bloom (*Chl*=0.2 mg m^{-3}) in the case of a clear (τ_a(865nm)=0.1) and moderately turbid (τ_a(865nm)=0.3) atmosphere, (b) polar diagram showing the geometry of multidirectional observations of the two selected targets. The solar zenith angle is 27°.

3.2.2 Validation at global scale

The second case considered for the validation of theoretical results using remotely sensed measurements consists in analysing a data set of PARASOL images covering a more global area than the regional study performed in section 3.2.a. The invariance of $\rho_{pol\_rc}(TOA)$ with water content is now examined using a set of images acquired at different periods of the year 2006 above the Atlantic Ocean along satellite overpasses covering the latitude range 60°N-60°S. The images were representative of the variability of oceanic contents that can be found in the Atlantic Ocean. Only targets viewed under a geometry for which simulations showed that $\Delta\rho_{pol\_rc}$ $(Chl=3.0\ mg\ m^{-3})$ is lower than PARASOL instrumental noise (see Fig. 1) were selected to compare measurements with theory. Based on the statistical analysis made in section 3.1 (table 1), these targets represent about 87% of the total number of targets observed along the satellite overpass. Targets showing similar atmospheric optical properties based on level 2 PARASOL geophysical products were analysed first. The values of the aerosol optical depth at 865 nm and Angstrom exponent were 0.1±0.003 and 0.17±0.02 respectively. To take into account and to respect the dependency of $\rho_{pol\_rc}(TOA)$ on the observation geometry, the images were partitioned into domains bounded by the azimuth, solar and viewing angles. The angular discretisation was 2 degrees. Such partitioning provided a grid. The standard deviation of $\rho_{pol\_rc}(TOA)$ was first calculated for each elements of the grid. Then, the standard deviations were averaged. The mean standard deviation considering all the selected targets showed a value of 8.44×10^{-4} (table 2), which is close to the noise equivalent polarized reflectance of PARASOL instrument. In addition, the mean standard deviation calculated for the unpolarized reflectance is largely higher, namely 4.27×10^{-3} (table 2), thus confirming that the water content in suspended particles is significantly variable for the selected targets. The standard deviation calculated relatively to targets for which atmospheric and oceanic properties were both variable showed a value of 1.58×10^{-3}, which is significantly greater than the instrumental noise of PARASOL.

These results indicate that when the atmospheric conditions are fixed and the chlorophyll *a* concentration is variable for each target, the variation in the polarized signal measured at the top of atmosphere in the visible band over open ocean waters is sufficiently weak (i.e., 8.44×10^{-4}) to remain undetectable from space remotely sensed data. In the meantime, changes in atmospheric conditions induce a significant variation in $\rho_{pol\_rc}(TOA)$ (i.e., 1.58×10^{-3}) which

#91057 - $15.00 USD Received 20 Dec 2007; revised 6 Feb 2008; accepted 13 Feb 2008; published 15 Apr 2008

could thus be used to detect aerosol optical properties (turbidity and spectral features). These PARASOL observations corroborate the simulations performed in section 2.2 which indicated that polarized top of atmosphere reflectance was at the same time invariant to marine signal and sensitive to atmospheric particles. The agreement between radiative transfer simulations and the statistical analysis performed on global scale satellite data is satisfactory, thus validating theory with measurements. Therefore, the PARASOL multiangle polarized measurements in the visible contain no detectable information on the phytoplankton content, but they are strongly dependent on aerosols loading for certain viewing geometries (see Fig. 3 and Fig. 7). The consideration of these measurements into satellite data processing should improve the aerosols determination and subsequently the performances of both atmospheric correction algorithms and derived ocean color geophysical products.

Table 2. Standard deviation of the polarized top of atmosphere reflectance $\rho_{pol\_rc}(TOA)$ measured by PARASOL for satellite overpasses covering the Atlantic Ocean. The latitude of the satellite overpasses ranges from 60°N to 60°S. Images were selected along the year 2006 to be representative of different water compositions. The mean standard deviation was calculated for two cases: (i) when targets are viewed for similar atmospheric conditions (i.e. aerosol optical depth at 865nm of 0.1 and angstrom exponent of 0.17) and (ii) when targets are viewed for variable atmospheric conditions. The water content in suspended matter is variable (the chlorophyll *a* concentration ranges from 0.02 to 7 mg m^{-3}). The number of targets used for each calculation of the mean standard deviation is 1000.

	Similar atmosphere	Variable atmosphere
Mean standard deviation of unpolarized reflectance $\rho_{rc}(TOA)$	4.27×10^{-3}	10.33×10^{-3}
Mean standard deviation of polarized reflectance $\rho_{pol\_rc}(TOA)$	8.44×10^{-4}	1.58×10^{-3}

4. Conclusion

In this paper, the sensitivity of the top of atmosphere multiangle and polarized reflectance in the visible spectrum to oceanic constituents was examined for open ocean waters and for a great variety of observation geometries. The first part of the study deals with theoretical computations using radiative transfer modelling. The simulations revealed that the polarized reflectance is virtually insensitive to phytoplankton biomass in any geometrical conditions when the chlorophyll *a* concentration is lower than 1 mg m^{-3} which represents about 90% of the global ocean. The invariance of the top of atmosphere signal with marine optical components was explained by the combination of the major contribution of atmospheric and air-sea interface effects to polarization signal together with the weak influence of phytoplanktonic cells on polarized radiation. In blooming conditions (i.e., $Chl > 3$ mg m^{-3}), despite a greater impact of oceanic particles on top of atmosphere polarized reflectance, our results showed that multidirectional acquisitions allow to find observation geometries for which the invariance property of TOA polarized reflectance is still verified. On the other hand, the variations observed in the polarized reflectance at 490 nm for such geometries are shown to be sufficiently significant to derive some information about the optical properties of aerosols and to discriminate between aerosol models. Therefore, the simulations showed that the multiangle and polarized reflectance collected in a visible band is a powerful tool that could be systematically used to separate between the estimation of oceanic and atmospheric optical properties over open ocean waters.

A rigorous approach was then conducted to validate the theoretical calculations. We focused on the practical application of theory to the sole satellite sensor that is currently able to measure the polarization and multidirectional features of the radiation exiting the ocean-atmosphere system, namely the PARASOL satellite instrument. First, a statistical analysis of geometries of observation exclusive to PARASOL sensor was performed to determine the degree of applicability of radiative transfer modelling computations for real world conditions.

#91057 - $15.00 USD Received 20 Dec 2007; revised 6 Feb 2008; accepted 13 Feb 2008; published 15 Apr 2008

The analysis showed that 87% of the targets viewed by PARASOL are observed under geometries for which predictions indicate that top of atmosphere polarized signal is insensitive to phytoplankton biomass. Second, PARASOL derived geophysical products such as atmospheric parameters and chlorophyll *a* concentration were used to test the property of invariance of TOA polarized signal with oceanic constituents. The PARASOL images were analysed at both regional and global scales. The regional scale study showed that the variations in the TOA polarized reflectance at 490 nm ρ_{pol_rc} are within the noise equivalent polarized reflectance of PARASOL instrument when the targets exhibited similar aerosol optical properties and strongly variable chlorophyll *a* concentrations. The variations in ρ_{pol_rc}, which were greater than the instrumental noise, were attributed to variations in aerosol optical properties. Similar results were obtained when the analysis was performed on a global area such as the Atlantic Ocean, thus providing a rigorous validation of theoretical predictions. PARASOL radiometric and polarimetric performance is sufficiently satisfactory to extract information on aerosols regardless of subsurface suspended matter optical properties in any conditions. This study allows to envisage the use of PARASOL polarized and multiangle data measured in the visible band to better constrain the aerosols detection and atmospheric correction algorithms over open ocean waters in order to improve the accuracy of retrieval of ocean color parameters such as the chlorophyll *a* concentration. Note that this is the first time, to our knowledge, that satellite polarized data acquired in a visible band are exploited for ocean color prospects. Since PARASOL is the sole sensor measuring the polarization and multidirectionality of the radiation, the development of other satellite sensors capable of measuring similar features from space is strongly encouraged in the future. Such sensors may include a greater number of visible polarized channels to gain an understanding on aerosols spectral optical properties and thus, on their impact on Earth's radiative budget.

Acknowledgments

This research was supported by Centre National d'Etudes Spatiales (CNES) and by ACRI-ST Company through the doctoral fellowship of Tristan Harmel. The authors would like to thank the organization ICARE (Laboratoire Optique Atmospherique and CNES) and the Hygeos Company for providing the PARASOL geophysical products. The authors also wish to thank the anonymous reviewers for their relevant comments and suggestions.

#91057 - $15.00 USD Received 20 Dec 2007; revised 6 Feb 2008; accepted 13 Feb 2008; published 15 Apr 2008